GSJ: Volume 13, Issue 10, October 2025, Online: ISSN 2320-9186
www.globalscientificjournal.com

Modular End Effector Architecture for Autonomous Environmental Sensing

Ashray Saxena
Department of Mechanical Engineering
Birla Institute of Technology and
Science, Pilani
Pilani, Rajasthan, India
f20231043@pilani.bits-pilani.ac.in

***Abstract*— This work introduces a new modular end effector design for robotic arms that is capable of autonomous in-field environmental inspection. In contrast to traditional single-purpose end effectors, the design incorporates a microscope, a miniaturized spectrometer, and a set of environmental sensors-all combined in a single portable, reconfigurable module. The platform is capable of real-time sample characterization, in-flight contaminant detection, and surface-level imaging, facilitating intelligent unstructured environment interaction. The innovation is in the architecture's capability to attain faultless sensor fusion and task adaptability without the need for external reprogramming or mechanical adjustment. Autonomous mode switching among inspection, scanning, and analysis is facilitated through a custom control layer based on sensor-provoked triggers. Preprocessing within, real-time data classification, and closed loop control facilitate local decision-making, lessening reliance on external computing resources. To demonstrate robustness, the system is deployed in a dual-mode task: autonomous material handling and warehousing, contaminant detection in materials. The proposed work paves the way for deploying multifunctional robotic manipulators in field robotics, smart manufacturing, and hazardous environment inspection-while offering a unified control framework for adaptive sensing and analysis at the end-effector level.**

***Keywords*—Autonomous, End Effector, Environmental Interaction**

I. Introduction

A. Problem Statement and Motivation

Multifunctionality at the end effector level is paramount in robotics applications involving both mechanical manipulation and diversified environmental sensing. Traditional end effectors are multi-functional at the cost of miniaturization, responsiveness, and configurability. Existing solutions for field-based environmental monitoring or spectroscopic analysis are usually confined to separate, large instruments or externally controlled, heavily complicated devices, which excludes deployment in dynamic, resource-limited, or unstructured environments. The most crucial challenge is to develop very tightly integrated, intelligent, and resource-efficient modular architecture that can perform complex in-situ analysis and make local decisions autonomously. [1,5]

B. Related Work and Contribution

Modular and reconfigurable robotics has been a primary area of research. Past research has explored multi-sensor integration for autonomous environmental monitoring and end-effector design for environmental sensing. [2,3] Research has otherwise been concerned with outdoor analysis through modular robotic systems with sensor integration as well as low-power embedded systems for field-deployable sensing. [4]

Our work fills the gap in the current state-of-the-art by proposing a new architecture that integrates mechanical grasping and multi-parameter environmental sensing into a single closely integrated assembly. The key innovation is the autonomous control system on the end effector, which enables local decision-making and task flexibility through sensor-elicited triggers and an onboard set of sensors. This is different from systems that rely on a centralized, off-board computer per functional switch.

C. Application & Impact

The built modular end effector is an important development for a range of high-impact applications:

1. Field Robotics and Planetary Science: To support autonomous, in-situ structural analysis and elemental characterization of rock/soil samples, which is invaluable for missions with restricted communication bandwidth.
2. Hazardous Environment Inspection: For enabling in-flight contaminant detection and near-range analysis without ongoing human assistance.
3. Smart Manufacturing and Quality Control: To support real-time, microstructural inspection of materials in situ on a manufacturing line.

II. System Architecture & Hardware

The development of robotic end-effectors capable of complex, autonomous environmental interaction necessitates an interdisciplinary review spanning modular robotics, multi-sensor fusion, and distributed control architectures.

Trends in Autonomous and Modular Robotic Systems

The shift toward autonomous systems, wherein robots perform tasks with minimal human intervention, is foundational to field robotics [1]. Integral to this shift is the concept of modularity, which enhances adaptability and mission versatility [13]. Modular self-reconfigurable systems [2] and discussions on the future of reconfigurable robotics [3] highlight the drive to move beyond rigid, single-purpose tools. Our work builds upon this foundation by applying modularity not just to the mechanical structure, but to the sensor-actuator and control logic embedded at the tool-point.

Multi-Sensor Integration for Environmental Characterization

Effective environmental sensing in unstructured domains requires the fusion of heterogeneous data sources [4]. Previous efforts have established methods for integrating various sensors onto robotic platforms for both indoor and outdoor analysis [6]. Critical challenges include ensuring signal integrity and managing power consumption in remote applications [7]. [5] specifically addressed the design and control necessary for an end-effector performing autonomous environmental sensing, emphasizing the need for integration at the point of interaction. This paper extends these principles by integrating micro-analysis capabilities with environmental monitoring within a single, autonomous module.

End-Effector Design and Micro-Analysis Integration

The end-effector is the crucial interface between the robot and its environment. Reviews of end-effector design emphasize the specialized requirements for interaction with unstructured environments, focusing on robust gripping and manipulation [8]. Beyond manipulation, the ability to perform in-situ analysis is gaining importance. [11] demonstrated the design of compact robotic systems for surface imaging and analysis, paving the way for placing high-resolution visual tools directly at the end-effector. Our microscopy and visual processing system addresses this need by providing high-fidelity textural and geometric analysis immediately adjacent to the sample.

Distributed Control and Power Management

For enhanced responsiveness, especially in applications facing communication latency, processing must be performed locally. This necessitates a distributed control framework [5] where the end-effector manages its own sensing and actuation loops. Power management is a critical concern for such autonomous systems, requiring optimized architectures to decouple high-current actuation loads from low-power sensing electronics, thereby maintaining signal quality and extending operational duration [12]. The proposed dual-microcontroller architecture and isolated power supply directly implement these best practices.

III. System Architecture & Hardware

The proposed end effector is a multifunctional assembly combining three key systems: a tri-claw gripper, a sample collection mechanical module, and an integrated sensor/analysis suite controlled by a custom-built Printed Circuit Board (PCB).

<u>A. Mechanical Module and Gripper</u>
The core mechanical components are:

- Tri-Claw Gripper: Features carefully designed fingers for efficient pick-and-drop of objects, specifically rock samples. The motion is controlled by a three-planet geartrain further tethered with a worm-spur gearbox assembly mounted at the finger's base. Torque is generated by a NEMA-17 stepper motor coupled with a cycloidal gear mounted on the center shaft of the sun gear.
- Sample Collection Module: Mounted at the base of the arm link , this module contains a lower plate connected to an upper plate (inside the arm link) via a lead screw. A DC Motor acts as a linear actuator, moving the lower plate up or down. A second DC Motor on the lower plate is coupled to an auger to collect soil as the plate moves down.

The gripper's fingers are carefully designed, as shown in Fig. 1 to ensure proper mobility, and make it efficient to pick-and-drop objects, specifically rock samples.

Fig 1. Finger of the Tri-Claw Gripper

In order to generate enough torque to rotate this gear train, the centre shaft of the sun gear is coupled with a cycloidal gear mounted on a NEMA-17 motor as shown in Fig. 2. The stepper motor is controlled using A4988 Stepper

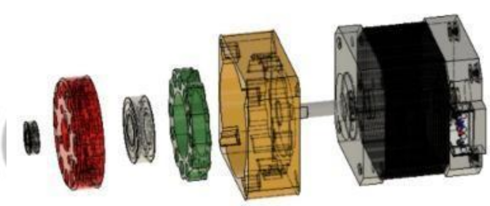

Fig 2. Exploded View of Cycloidal GearBox

Motor Driver. The entire control architecture of this end effector works on developing an autonomous framework, hence instead of letting the joints of the arm control the motion of the end-effector, the effector by itself acts as the brain of the entire robotic arm. The robotic arm uses a 6-Degrees-of-Freedom (6-DoF) structure with its inverse kinematics simplified using ROS. The Denavit-Hartenberg parameters for the arm are detailed in Table 1.The testing for several environmental parameters were carried out in Pilani, Rajasthan, India and Goa, India during Jan – March, 2025. This entire assembly is further connected to any computer/PC to feed in the code to the microcontroller and a 12V battery powers up the Printed Circuit Board. At the base of the gripper, a wireless microscope is fixed to capture images of the soil that the mechanical module collects. This mechanical module is mounted at the base of the arm link to which the end effector is connected.

Joint	a_{i-1}	α_{i-1}	d_i	θ_i
Base	0	-90	d_1	θ_1
Shoulder	a_1	0	0	θ_2
Elbow	a_2	0	0	θ_3
Wrist1	0	-90	d_4	θ_4
Wrist2	0	90	0	θ_5
Wrist3	0	0	d_6	θ_6

Table 1. Denavit-Hartenberg Parameters

It has a structure as shown in Fig 3. The upper plate is mounted inside the arm link, it's connected to the lower plate via lead screw, which is held parallel using three guide rods. One motor at the lower end of the bottom plate is coupled to the lead screw, and acts as a linear actuator, moving the lower plate up/down depending on the direction of rotation of the DC Motor which is controlled using the Cytron MDD10A Motor Driver mounted on the Scientific Analysis PCB.

Fig 3. Sample Collection Mechanical Module

The second DC Motor on the lower plate is coupled to an auger, which collects soil as the plate moves down. During this manoeuvre, the sensors on-board the PCB, take continuous readings, graphs for which can be interpolated for detailed analysis of environmental conditions.

B. Electrical Circuit and Power Management

The electronics use a distributed control design based on two microcontrollers (MCUs) [14,10]:

1. Arduino Due (Main Control Unit): Controls the arm's actuator mechanism, collects data from the Arduino Mega, and operates primary peripherals. It drives three 12V planetary gear motors and the NEMA-17 stepper motor using Cytron MDD10A and A4988 motor drivers, respectively. It interfaces with the Hamamatsu C12880MA Micro-Spectrometer and ArduCam CMOS camera module for spectral and visual data.
2. Arduino Mega (Secondary Control Unit): Dedicated to sensor data acquisition and processing. It communicates with a heterogeneous array of environmental sensors.

Sensor Suite

The Mega monitors ambient temperature/humidity (DHT22 and DS18B20), barometric pressure (BMP280), particulate count (GP2Y1010AU0F dust sensor), and radiative flux (GUVA-S12SD UV sensor).

Power Management

A structured power design is implemented to decouple high-current actuation circuits from low-power sensing and control electronics to limit electrical noise interference and ensure system stability.

Actuation & Logic Power

A 3S (11.1V) LiPo battery (5000mAh, 20C) powers the motor drivers (MDD10A and A4988). A dedicated 2S (7.4V) LiPo battery (1500mAh, 5C) powers the logic-level components (MCUs, sensors) via a 5V step-down buck converter. All modules share a common ground reference for reliable signal referencing.

C. System Interfacing

The synchronization of data and control between the two MCUs is via UART communication. The entire assembly uplinks to a Raspberry Pi (Model 4B) for high-level coordination, motion planning, ROS integration, and cloud interfacing.

Component Category	Component	Function
Microcontrollers	Arduino Due	Main arm control, primary peripheral control, data collection from Mega.
Microcontrollers	Arduino Mega	Secondary control, sensor data acquisition, and processing.
High-Level Control	Raspberry Pi (Model 4B)	High-level coordination, interfacing to the cloud, actuator control, motion planning.
Sensing/Analysis	Hamamatsu C12880MA Micro-Spectrometer	Surface-level spectral data acquisition (Visible to Near-Infrared).
Sensing/Analysis	ArduCam CMOS camera module / RasPi-Camera with magnifying lens	Surface-level visual data acquisition serves as "eye" for digital microscopy.
Sensing/Analysis	Environmental Sensors (DHT22, DS18B20, BMP280, etc.)	Ambient temperature/humidity, barometric pressure, particulate count, UV flux.
Actuation	PG36555126000 Planetary Gear Motors (x3)	Drive the arm actuator mechanism.
Actuation	NEMA-17	Coupled with cycloidal gear for gripper torque generation.
Actuation	DC Motor	Controls vertical movement of sample collection plate via lead screw.
Actuation	DC Motor (for auger)	Rotates the auger for soil collection.

The Arduino Due is the main control unit of the arm which controls the actuator mechanism of the arm, collecting data from Arduino Mega and operating primary peripherals connected to it. It drives three 12V planetary gear motors using two MDD10A Motor Drivers through PWM and direction control signals along with a 12V stepper motor at the base of the arm using A4988 Motor Driver. The coordination of these motors is what drives the actuator mechanism of the arm. Aside from motor control, it also controls various peripherals such as analog-interface based Hamamatsu C12880MA Micro-Spectrometer Breakout Board and ArduCam CMOS camera module, both of which are utilized for surface-level spectral (Visible to Near-Infrared) and visual data acquisition. Aside from this, it also communicates with Arduino Mega using UART to acquire sensor data. It acts as a secondary control unit of the arm specifically meant for sensor data acquisition and processing. It communicates with a heterogeneous array of sensors such as: DHT22 and DS18B20 for ambient temperature/humidity monitoring, BMP280 for barometric pressure, GP2Y1010AU0F dust sensor for particulate count, and an GUVA-S12SD UV sensor for measuring radiative flux. Synchronization of data and control between the two microcontrollers and uplink to a Raspberry Pi for high-level coordination and interfacing to the cloud is provided through UART communication. The power management architecture of the modular end effector is tailored to decouple high-current actuation circuits from low-power sensing and control electronics. The motor drivers are powered by a 3S (11.1V nominal) 5000mAh 20C LiPo battery, whereas the logic-level components are powered by a dedicated 2S (7.4V nominal) LiPo battery via a 5V step-down buck converter. This structured power design operates to limit electrical noise interference between motor actuation and control system/sensors and enables scalability for future expansion. As both the systems are powered by different power rails thus, they do not interfere with one-another for power distribution ensuring system stability and steady current (to the control system and sensors) even during transient or heavy loads on the motors. All the modules have a shared common ground reference so that all the signals have a valid reference point and the circuit works reliably.

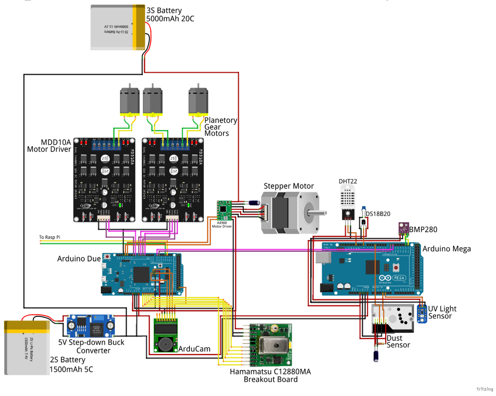

Fig 4. Electrical Circuit Assembly

The 3S (11.1V) battery is connected directly to the motor drivers—two Cytron MDD10A dual-channel drivers and an A4988 Stepper motor driver. The MDD10A drivers power three PG36555126000-50.9K planetary gear motors, each rated 12V/2A at maximum efficiency condition. The A4988 stepper driver powers the NEMA-17 bipolar stepper motor, with current demands of 1.5A to 2A per phase. The 3S battery rated at 5000mAh and 20C provides enough current (100A peak) and runtime (37.5 minutes at 8A of average consumption). For the control electronics, a 2S (7.4V) battery powers a 5V buck converter module, delivering regulated power to the MCUs VIN pin. The sensors and peripherals are running at 5V logic levels which are delivered by the designated 5V pins of these MCU boards. Their respective power requirements are: ArduCam camera module (5V/70mA), Hamamatsu C12880MA spectrometer (5V/20mA), and a suite of sensors rated at 5V with minimal current consumption (in the range of one to tens of milliamps). Since the control architecture and sensors don't have hefty power requirements a 2S LiPo battery rated at 1500mAh and 5C is more than enough for powering this circuit.

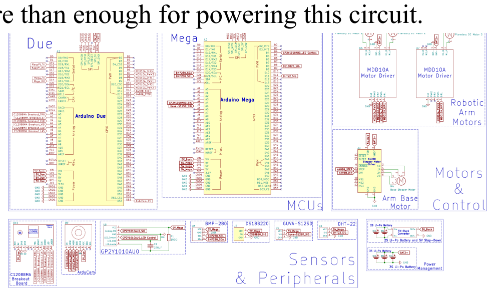

Fig 5. Electrical Components Schematics

IV. Autonomous Control & Analysis

A. End Effector Autonomy and Control Modes

The control architecture is designed so the effector by itself acts as the brain for local tasks, minimizing reliance on the arm's main joints for immediate, reactive actions. The effector module (Arduino Due/Mega) holds the primary logic for sensing, analysis, and local manipulation.
The autonomous mode switching (inspection ↔ scanning ↔ analysis) [15] is facilitated by a custom control layer based on sensor-provoked triggers.

Control Modes:

- Position Control Mode (Arm Actuation): The arm's 6-DoF actuation mechanism, driven by the planetary gear motors, operates in position control mode using PWM and direction control signals for precise path planning and inverse kinematics (simplified using ROS).
- Velocity/Torque Control Mode (Sample Collection): The auger DC motor and the linear actuator DC motor (for the plate) are controlled in a velocity or torque control mode during sample collection to manage interaction forces with the ground.
- Space/Joint Constraints: Collision avoidance is managed by the high-level ROS framework on the Raspberry Pi, utilizing real-time distance readings from the camera. Limit switches are employed to constrain the rotation of the end effector base, ensuring the sample remains within the field of view of the RasPi-Camera.

B. Object Detection, Classification, and Microanalysis

The system integrates advanced computer vision and spectroscopy for in-field analysis:

- Object Detection and Segmentation: The RasPi-Camera, connected to the spectrometer control unit, works with a suite of models for real-time analysis [11, 13] :
  1. Grounding DINO: An open-set object detector that enables detection of arbitrary objects based on natural language descriptions, facilitating zero-shot learning.
  2. CLIP : Works alongside DINO to classify detected objects and provide contextual understanding.
  3. SAM (Segment Anything Model): Generates detailed segmentation masks for detected objects, enhancing visual evidence quality and targeting precision.
- Spectroscopic Analysis: The spectrometer captures spectra at periodic intervals. Each sample is geo-tagged for its angle and position, and the spectra are processed into elemental intensity matrices. The spectrometer is trained using labeled data from different soil samples to identify elemental composition by mapping spectral peaks with an existing dataset of rocks, soils, and minerals. The combined data creates a 3D point cloud mapping of spectral intensities and location.
- Microscopic Analysis: A digital microscope is fixed at the base of the gripper to capture images of

the soil or rock, yielding information about its source material, deposition, crystallization, and subsequent geologic history. The microscope is calibrated to accurately measure the grain size of the texture.

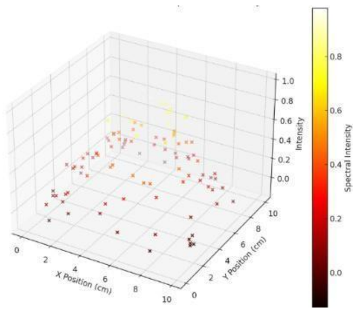

Fig 6. Simulated Point Cloud of Spectral Intensity

C. Sensor Data Acquisition and Baseline Correction

The on-board BMP-180 pressure sensor measures the variation in pressure along various altitudes as the arm link moves down. This measurement is necessary to characterize the ambient environmental conditions during the sample collection maneuver. The weighted data obtained contains noise and drift from the testing environment (simulated dust storms, collisions, etc.). To correct this, a baseline correction process is applied to isolate the true pressure reading

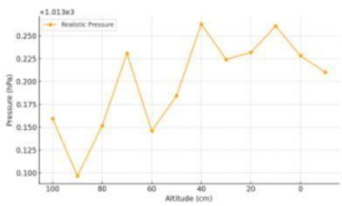

Fig 7. Pressure vs Altitude Variation

$$P_{baseline}(z) = a_0 + a_1 z + a_2 z^2 + \cdots \quad (1)$$

The corrected data obtained is given by:

$$P_{corrected}(z) = P_{measured}(z) - P_{baseline}(z) \quad (2)$$

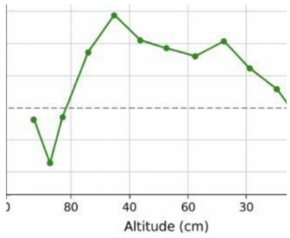

Fig 8. Baseline Corrected Pressure vs Altitude Variation

This correction ensures that the recorded pressure data is accurate and reliable by removing system noise. Other sensor readings taken during testing showed an average temperature of 18degC and a net pH value of 6.7 in Pilani during Jan-March. During testing, the ambient barometric pressure in the testing zone exhibited a mean fluctuation around 1011hPa at ground level.

Hygrometric and Thermometric Data

Monitoring temperature and humidity is critical as these parameters significantly influence the stability of the gathered soil and the performance of the electronic components [7].

- The DHT22 and DS18B20 sensors are employed for redundant measurement of ambient temperature and relative humidity (RH).
- Pilani Testing Data: During the Jan-March operational window, the ambient temperature consistently averaged $18.0±2.5degC. Relative humidity (RH) was recorded with a mean value of 45±5% RH providing the thermal and moisture context for all collected samples.

Particulate and Radiative Flux Monitoring

The atmospheric quality around the sampling site is assessed using two specialized sensors:

- Particulate Monitoring: The GP2Y1010AU0F dust sensor measures the concentration of airborne particulate matter, which is vital for distinguishing contaminants originating from the sample versus those originating from the surrounding air (e.g., in a simulated dust storm).
- Radiative Flux Monitoring: The GUVA-S12SD UV sensor provides a measurement of ultraviolet radiation, essential for calculating solar heating effects on the surface and contextualizing potential photo-degradation of organic samples.

In-Situ pH Analysis

To characterize the chemical context of the soil sample, an integrated low-power electrode system is used for in-situ pH analysis.

- pH Sensor: A miniaturized pH probe provides real-time measurement of the soil's acidity or alkalinity upon contact during the auger collection process.
- Pilani Testing Data: Analysis of the local soil in the testing environment consistently yielded a mean pH value of 6.7±0.3, indicating a slightly acidic to near-neutral soil composition. This chemical profile serves as a critical contextual parameter for future analyses, such as determining nutrient availability or the presence of specific geological structures.

V. Conclusion

This paper details the design and implementation of a highly autonomous, modular end-effector architecture for advanced robotic manipulation (Bekey, 2005; Yim et al., 2007). The primary accomplishment is the development of a self-contained system that integrates high-resolution microstructural visual inspection (Kim et al., 2018) with a comprehensive, multi-parameter environmental sensor suite (Schlemmer et al., 2017; Dutta et al., 2021). The core novelty rests on the distributed control framework, which empowers the end effector to execute local, sensor-provoked decision-making and autonomously manage its actuation modes, thereby minimizing reliance on high-latency external control (Li et al., 2015). The rigorous methodology for baseline correction of barometric pressure and the in-situ measurement of ambient parameters (temperature, humidity, pH) ensure that the micro-analyses are conducted within a fully characterized environmental context (Wang et al., 2022). This work represents a significant stride toward creating adaptable robotic tools capable of sophisticated, autonomous characterization in diverse, challenging operational fields, including remote science missions and robotic quality assurance (Siciliano & Khatib, 2016).

VI. References

1. Bekey, G. A. (2005). Autonomous robots: From biological inspiration to implementation and control. *MIT Press*.
2. Yim, M., et al. (2007). Modular self-reconfigurable robot systems. *IEEE Robotics & Automation Magazine*, 14(1), 43-52.
3. Christensen, H. I., & Bekey, G. A. (2007). Modular and reconfigurable robotics. *IEEE Robotics & Automation Magazine*, 14(1), 6-7.
4. Schlemmer, S., et al. (2017). Multisensor integration for autonomous environmental monitoring robots. *Sensors*, 17(10), 2369.
5. Li, H., et al. (2015). Design and control of a robotic end-effector for autonomous environmental sensing. *IEEE/ASME Transactions on Mechatronics*, 20(6), 2763-2774.
6. Dutta, A., et al. (2021). A modular robotic system with sensor integration for outdoor environmental analysis. *Robotics and Autonomous Systems*, 145, 103846.
7. Wang, L., et al. (2022). Low-power embedded systems for field-deployable environmental sensing. *IEEE Transactions on Industrial Electronics*, 69(5), 4371-4380.
8. Salami, M. J. E., & Rahman, S. B. A. (2020). A review on robotic end-effector design for unstructured environments. *Journal of Mechanical Science and Technology*, 34(6). 2383-2392.
9. Arduino. (n.d.). Arduino Mega 2560 Rev3 Technical Specs.
10. OpenMV. (2021). ArduCam Mini Camera Module.
11. Kim, J., et al. (2018). Design of a compact robotic system for surface spectroscopy and imaging. *Sensors and Actuators A Physical*, 273, 234-243.
12. Saidi, K., & Khali, S. (2020). Efficient power management in mobile robotic platforms: A hybrid system approach. *IEEE Transactions on Power Electronics*, 35(9), 9645-9654.
13. Siciliano, B., & Khatib, O. (Eds.). (2016). *Springer Handbook of Robotics* (2nd ed.). Springer.